

Article

# A Novel Potent Crystalline Chitin Decomposer: Chitin Deacetylase from *Acinetobacter schindleri* MCDA01

Guang Yang<sup>1,2,3,4</sup> , Yuhan Wang<sup>1,4</sup>, Yaowei Fang<sup>1,2,3,4</sup>, Jia An<sup>1,4</sup> , Xiaoyue Hou<sup>1,2,3,4</sup>, Jing Lu<sup>1,2,3,4</sup>, Rongjun Zhu<sup>1,4</sup> and Shu Liu<sup>1,2,3,4,\*</sup>

<sup>1</sup> Jiangsu Key Laboratory of Marine Bioresources and Environment, Jiangsu Ocean University, Lianyungang 222005, China

<sup>2</sup> Co-Innovation Center of Jiangsu Marine Bio-Industry Technology, Jiangsu Ocean University, Lianyungang 222005, China

<sup>3</sup> Jiangsu Marine Resources Development Research Institute, Jiangsu Ocean University, Lianyungang 222000, China

<sup>4</sup> College of Food Science and Engineering, Jiangsu Ocean University, Lianyungang 222005, China

\* Correspondence: jdliushu@163.com; Tel./Fax: +86-05-15861246008

**Abstract:** Chitosan is a functional ingredient that is widely used in food chemistry as an emulsifier, flocculant, antioxidant, or preservative. Chitin deacetylases (CDAs) can catalyze the hydrolysis of acetyl groups, making them useful in the clean production of chitosan. However, the high inactivity of crystalline chitin catalyzed by CDAs has been regarded as the technical bottleneck of crystalline chitin deacetylation. Here, we mined the *AsCDA* gene from the genome of *Acinetobacter schindleri* MCDA01 and identified a member of the *uraD\_N-term-dom* superfamily, which was a novel chitin deacetylase with the highest deacetylation activity. The *AsCDA* gene was expressed in *Escherichia coli* BL21 by IPTG induction, whose activity to colloidal chitin,  $\alpha$ -chitin, and  $\beta$ -chitin reached 478.96 U/mg, 397.07 U/mg, and 133.27 U/mg, respectively. In 12 h, the enzymatic hydrolysis of *AsCDA* removed 63.05% of the acetyl groups from  $\alpha$ -chitin to prepare industrial chitosan with a degree of deacetylation higher than 85%. *AsCDA*, as a potent chitin decomposer in the production of chitosan, plays a positive role in the upgrading of the chitosan industry and the value-added utilization of chitin biological resources.

**Keywords:** chitin deacetylase; crystalline chitin; *Acinetobacter schindleri*; *uraD\_N-term-dom* superfamily; chitosan



**Citation:** Yang, G.; Wang, Y.; Fang, Y.; An, J.; Hou, X.; Lu, J.; Zhu, R.; Liu, S. A Novel Potent Crystalline Chitin Decomposer: Chitin Deacetylase from *Acinetobacter schindleri* MCDA01. *Molecules* **2022**, *27*, 5345. <https://doi.org/10.3390/molecules27165345>

Academic Editor: Hong Jiang

Received: 15 July 2022

Accepted: 17 August 2022

Published: 22 August 2022

**Publisher's Note:** MDPI stays neutral with regard to jurisdictional claims in published maps and institutional affiliations.



**Copyright:** © 2022 by the authors. Licensee MDPI, Basel, Switzerland. This article is an open access article distributed under the terms and conditions of the Creative Commons Attribution (CC BY) license (<https://creativecommons.org/licenses/by/4.0/>).

## 1. Introduction

Chitin, a linear homopolymer of  $\beta$ -1,4-glycosidically linked N-acetylglucosamine (GlcNAc) residues, is the second largest natural polymer renewable resource after cellulose. Some 6 to 8 million tons of chitin solid waste are generated during the fishery processing of crab, shrimp, and lobster, which are value-added processing by-products of aquatic foods [1–3]. However, natural chitin has a dense crystalline structure, a highly ordered three-dimensional network, and a high degree of polymerization and insolubility in regular solvents, which severely limits the development and commercial application of chitin [4–6]. Therefore, natural chitin bioresource is often considered to be a burdensome waste product of the marine and biotechnology industries [7]. Chitosan, the deacetylated derivative of chitin, prepared from natural chitin sources with a degree of deacetylation higher than 55%, is widely used in the food industry, medicine, environmental protection, and agriculture due to its safety, non-toxic, biodegradable, biocompatibility, anti-oxidation, and bacteriostatic properties [8–10]. Significantly, chitosan is most widely used in the food industry, and these characteristics and the chemical structure of chitosan may contribute to its functionality and application as an emulsifier, flocculant, antioxidant, or preservative in

food chemistry. Meanwhile, chitosan preparations have been accepted as food additives and functional food ingredients in China, Japan, and Korea.

Chitin deacetylases (CDAs, EC 3.5.1.41) catalyze the deacetylation of chitin to prepare chitosan and chitin nanofibers to realize the value-added utilization of chitin biological resources [2,11,12]. Compared to the traditional physical and chemical methods to prepare chitosan from chitin, the bio-enzymatic production process treated by microbial CDAs has the advantages of safety, controllability, an environmentally friendly process, and high efficiency [13]. Significantly, the production of chitosan by this enzymatic process of CDAs resulted in a higher molecular weight, homogeneous end products, and the desired degree of acetylation, which is more useful in food chemistry and has a higher economic value [14]. Chitin deacetylases, classified in the carbohydrate esterase family 4 (CE4), were mostly reported in fungi and some insect species, and seldom reported in bacteria. Since the CDA from *Mucor rouxii* (MrCDA) was first discovered in 1975, CDAs have been studied in terms of fermentation optimization, physical and chemical properties, development and application, structure, and function [15–17].

Previous studies have reported only eight CDAs from microbial sources that catalyze the deacetylation of crystalline chitin (see Supplementary Table S1) [7,11,18–20]. These CDAs with low activity catalyzing crystalline chitin were the bottlenecks that limited the industrial production of chitosan by CDA enzymatic hydrolysis. CDAs with high activity on crystalline chitin can meet the demand for the industrial production of chitosan by enzymatic treatment. To obtain better accessibility to the acetyl groups for the deacetylation, natural chitin was pretreated and modified through various physical and chemical methods such as sonicating, grinding, heating, derivatization, and interaction with saccharides [21,22]. A variety of methods have been studied on improving the efficiency of enzymatic hydrolysis to crystalline chitin [19,23–27]. CDAs are, however, currently commercially unavailable. Therefore, the identification of a bacterial CDA with high activity on crystalline chitin should be explored to enzymatically convert it into chitosan.

*Acinetobacter schindleri* MCDA01 was screened producing the highest enzyme activity of wild CDA enzyme with 201.37 U/mL, which had a high efficiency of enzymatic hydrolysis to crystalline chitin for preparation of chitin nanofibers with significantly increased length and width by catalytic crystal chitin [11]. Although the wild CDA from *A. schindleri* MCDA01 has recently been enzymologically characterized, the genome sequence of *A. schindleri* MCDA01 and the gene sequence of its CDA are still unclear. Meanwhile, the activity of CDA from *A. schindleri* MCDA01 toward crystalline chitin has not yet been evaluated. In the present study, the genomic DNAs of *A. schindleri* MCDA01 were sequenced and analyzed, and the CDA gene (*AsCDA*) was mined based on the genomic analysis. The characterization and application of *AsCDA* toward crystalline chitin were evaluated. The preparation system of chitosan by the enzymatic method of *AsCDA* was constructed, which will play a positive role in the chitosan industrial technology upgrade and quality improvement. This study will perfect the enzymatic basis for the clean product of chitosan by CDAs and provide an experimental basis for the molecular mechanism of the deacetylation of crystalline chitin catalyzed by *AsCDA*.

## 2. Results and Discussion

### 2.1. General Genomic Features of the *A. schindleri* MCDA01 Strain

*Acinetobacter schindleri* MCDA01 has been reported to produce CDAs with higher activity for the preparation of chitin nanofibers with a notable increase in length and width by catalytic crystal chitin [11]. The purification process of the wild enzyme of CDA from *A. schindleri* MCDA01 is complex and the enzyme activity is seriously lost. This study focused on the clean production of chitosan through recombinant CDA from *A. schindleri* MCDA01 catalyzed chitin deacetylation, which will enhance the chitosan industrial technology upgrade and quality improvement. Consequently, the genome of *A. schindleri* MCDA01 was sequenced and analyzed to further research and acquire in-depth genomic level insights related to its molecular evolutionary, functional metabolite,

and biosynthetic potential. Sequencing the whole genome of the *A. schindleri* MCDA01 strain showed that the total length of the genome was 3.33 Mb (including the plasmid genome 0.17 Mb) with 43% GC content (see Supplementary Figure S1). The whole genome of *A. schindleri* MCDA01 encoded 3107 putative predicted genes, which were 84.31% of the genome sequence including 21 ribosomal rRNAs, 88 tRNAs, and 9 sRNAs (Table 1). The function annotation of putative CDs was successfully performed on 1902 GO genes (61.21% of the genome sequence, Figure 1A), 1881 KEGG genes (60.57% of the genome sequence, Figure 1B), 2267 COG genes (72.96% of the genome sequence, Figure 1C), and 35 CAZy genes (1.12% of the genome sequence, Figure 1D). To further analyze whether the *A. schindleri* MCDA01 strain was a potential chitin decomposer, chitin degrading enzymes involved in chitin deacetylation and hydrolysis were identified by the CAZy database. The 11 genes were annotated as deacetylases or chitinases including five gene-encoding chitinases and six gene-encoding deacetylases (including AsCDA) (see Supplementary Table S2), which were annotated for carbohydrate metabolic processes and catalytic and hydrolase activity toward carbon–nitrogen. The genome size, GC content, and CD quantity of *A. schindleri* MCDA01 were larger than other reported strains of *A. schindleri*, which may mean that more genes of the *A. schindleri* MCDA01 genome involved in the microbial metabolism process could adapt to different environmental conditions (see Supplementary Table S3) [28].

**Table 1.** General characteristics of the *Acinetobacter schindleri* MCDA01 genome.

General Features	<i>A. schindleri</i> MCDA01
Genome size (bp)	3,332,387
GC content (%)	43
Gene number	3107
Gene length	2,809,674
% of Genome (genes)	84.31
Gene average length	904.3
rRNAs	21
tRNAs	88
sRNAs	9
CAZy assignment	35
COG assignment	2267
GO assignment	1902
KEGG alignment	1881

## 2.2. Comparative Genome Analysis of *Acinetobacter schindleri* MCDA01

To investigate the evolutionary specificity and diversity of *A. schindleri* MCDA01, we carried out a comparative genomic analysis of different strains. Comparative genomics analysis revealed that *A. Schindleri* MCDA01 has few homologous genes with *B. anthracis* Ames and *B. cereus* ATCC14579, but more homologous genes with *A. schindleri* CIP107287 and *A. schindleri* ACE (Figure 2A) and these results were largely consistent with the previous study of Ye et al. [11]. Particularly, 418 genes (13.45% of the genome sequence) were shared, and unique genes of *A. schindleri* MCDA01 strain (Figure 2B) were involved in signaling and cellular processing, genetic information processing, carbohydrate metabolism (including AsCDA), lipid metabolism, environmental information processing, glycan biosynthesis and metabolism, amino acid metabolism, and so on (Figure 2C), which displayed that *A. Schindleri* MCDA01 has higher carbohydrate metabolism activity and is a potent chitin decomposer [29,30].

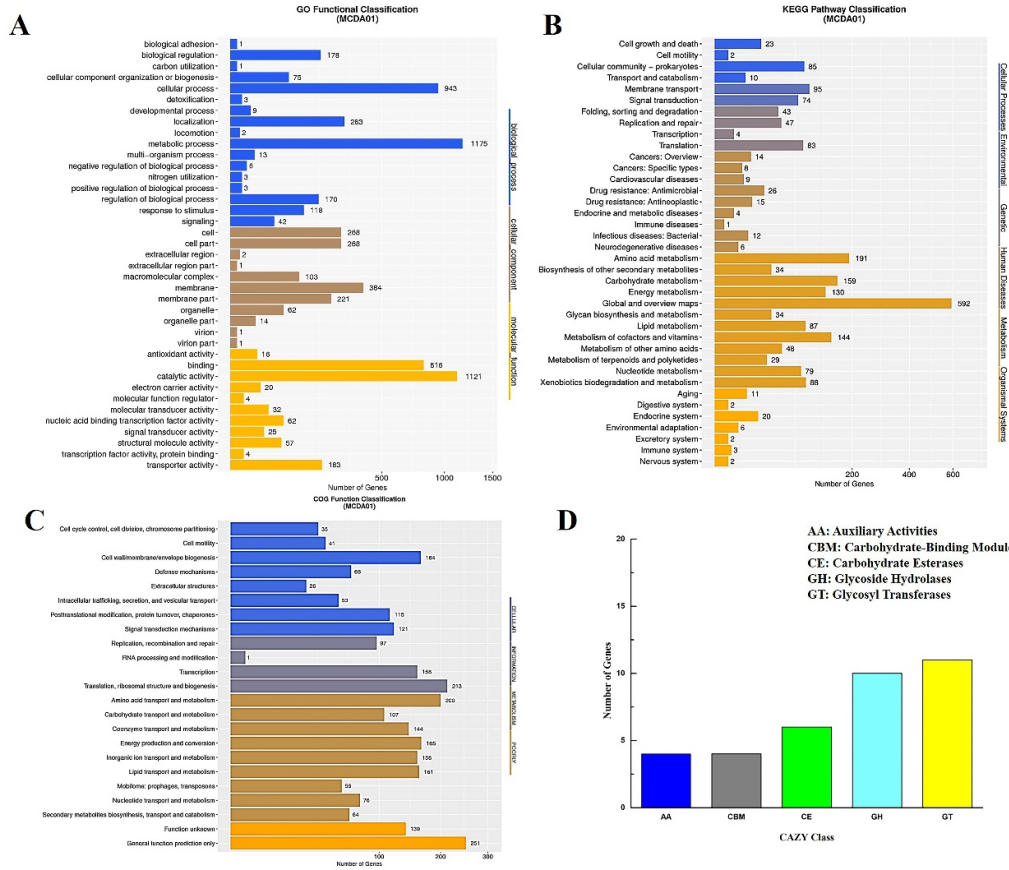


**Figure 1.** Genome analysis of *Acinetobacter schindleri* MCDA01: (A) Histogram showing the distribution of Gene Ontology (GO) terms; (B) Eucaryotic Orthologous Groups (COG) functional gene classification; (C) The Kyoto Encyclopedia of Genes and Genomes (KEGG) function annotation; (D) Carbohydrate-Active Enzymes (CAZy) family distribution map.

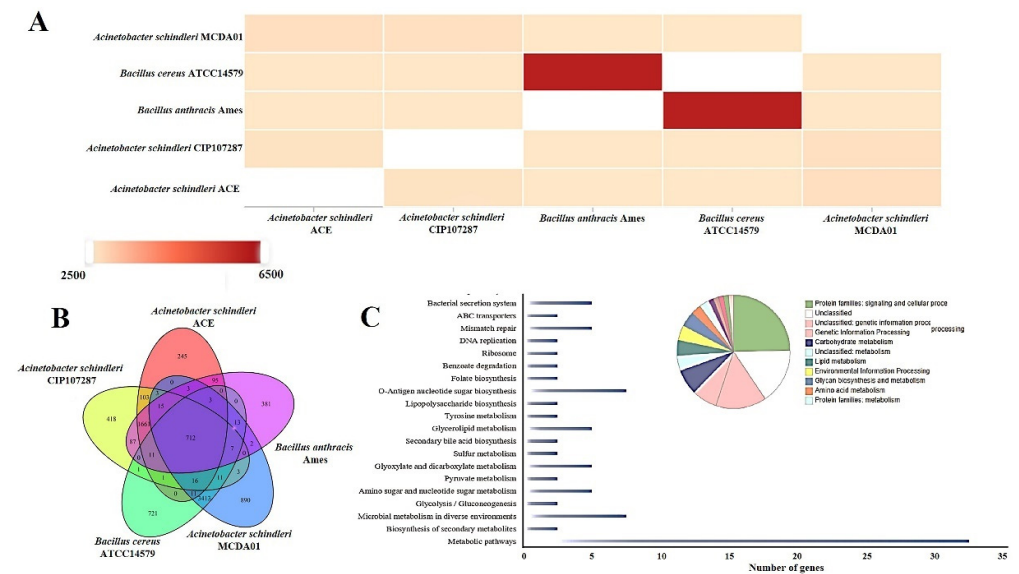


**Figure 2.** Comparative genome analysis of *Acinetobacter schindleri* MCDA01, *Acinetobacter schindleri* CIP107287, *Acinetobacter schindleri* ACE, *Bacillus anthracis* Ames, and *Bacillus cereus* ATCC14579: (A) similarity relations of genomes between four strains; (B) unique genes of the genomes of four strains; (C) KEGG pathway classification of these unique genes from the genome of *Acinetobacter schindleri* MCDA01.

### 2.3. Genome Mining and Bioinformatics Analysis of AsCDA

There are four genes annotated deacetylases belonging to the CE4 family in the *A. schindleri* MCDA01 genome database, and AsCDA was mined uniquely according to the molecular mass 31 kDa of natural chitin deacetylase [11]. The sequences of AsCDA were uploaded to GenBank with Accession NO. MW295944.1, but not opened. The AsCDA gene is a 975 bp encoding 324 amino acids with a Polysacc\_deac\_1 domain. To further determine the phylogenetic status of AsCDA, we performed a multiple sequence alignment, phylogenetic analysis, and homologous modeling of the AsCDA amino acid sequence with other 14 members of the deacetylase superfamily. The phylogenetic analysis identified these deacetylases from three different clades representing the CE4 superfamily, spore\_pdaA superfamily, and uraD\_N-term-dom superfamily, respectively [31,32]. AsCDA is clustered together with other members of the uraD\_N-term-dom superfamily and has high sequence similarity with *Schizosaccharomyces pombe* SpCDA, polysaccharide deacetylase from *Pseudomonas aeruginosa*, CDA from *Rhodococcus equi* F6, and PuuE protein from *Pseudomonas fluorescens*, some of which had enzymatic hydrolysis to chitooligosaccharides or chitin pretreated by [TBA][OH] (Figure 3A) [31,32]. Interestingly, multiple sequence alignment of these enzymes revealed that AsCDA has a few notable differences from other CDAs of the CE4 superfamily. The conserved Asp-His-His metal-binding triad of the CE4 family is replaced by Glu-His-Trp of AsCDA (active sites: Glu<sup>51</sup>, Glu<sup>52</sup>, His<sup>140</sup>, Trp<sup>144</sup>, and His<sup>276</sup>; Glu<sup>51</sup>: base catalytic site; His<sup>276</sup>: acid catalytic site, and the catalytic amino acid residues are different, with Glu replacing Asp for the acidic amino acid) (Figure 3B). Two conserved inserted segments (IS1 and IS2) of the AsCDA sequence do not have a counterpart in the CE4 superfamily (Figure 3B). In the next section, we will analyze the crystal structure of AsCDA to explore and elucidate the enzymatic reaction mechanism of this arrangement in the AsCDA sequence. Importantly, these results indicate that AsCDA is a new PuuE homolog of the uraD\_N-term-dom superfamily and has a high-enzyme activity to catalyze crystalline chitin deacetylation.

### 2.4. Heterologous Expression of AsCDA in *Escherichia coli*

The recombinant plasmid pET-28a-AsCDA was a heterologous expression in *E. coli* BL21. SDS-PAGE analysis showed that the molecular weight of purified AsCDA was approximately 37.5 kDa with 2.11 mg/mL by nickel affinity chromatography (Figure 4A), which was expected on the MW of natural chitin deacetylase produced by *A. schindleri* MCDA01. Some previous studies observed that the MW of chitin deacetylases ranged from 15 to 100 kDa and most chitin deacetylases were in the range of 35–40 kDa [8,14,22,33,34]. The specific activity of purified AsCDA treated colloidal chitin,  $\alpha$ -chitin and  $\beta$ -chitin were 478.96 U/mg, 397.07 U/mg, and 133.27 U/mg by acetic acid assay kit, respectively (Figure 4B). Previous results have shown that most CDAs had a high activity on chitooligosaccharides, water-soluble chitosan, and colloidal chitin, but low or no activity toward crystalline chitin [2,30]. Thus, AsCDA has potential application in the effective deacetylation of crystalline chitin substrates, especially  $\alpha$ -chitin.

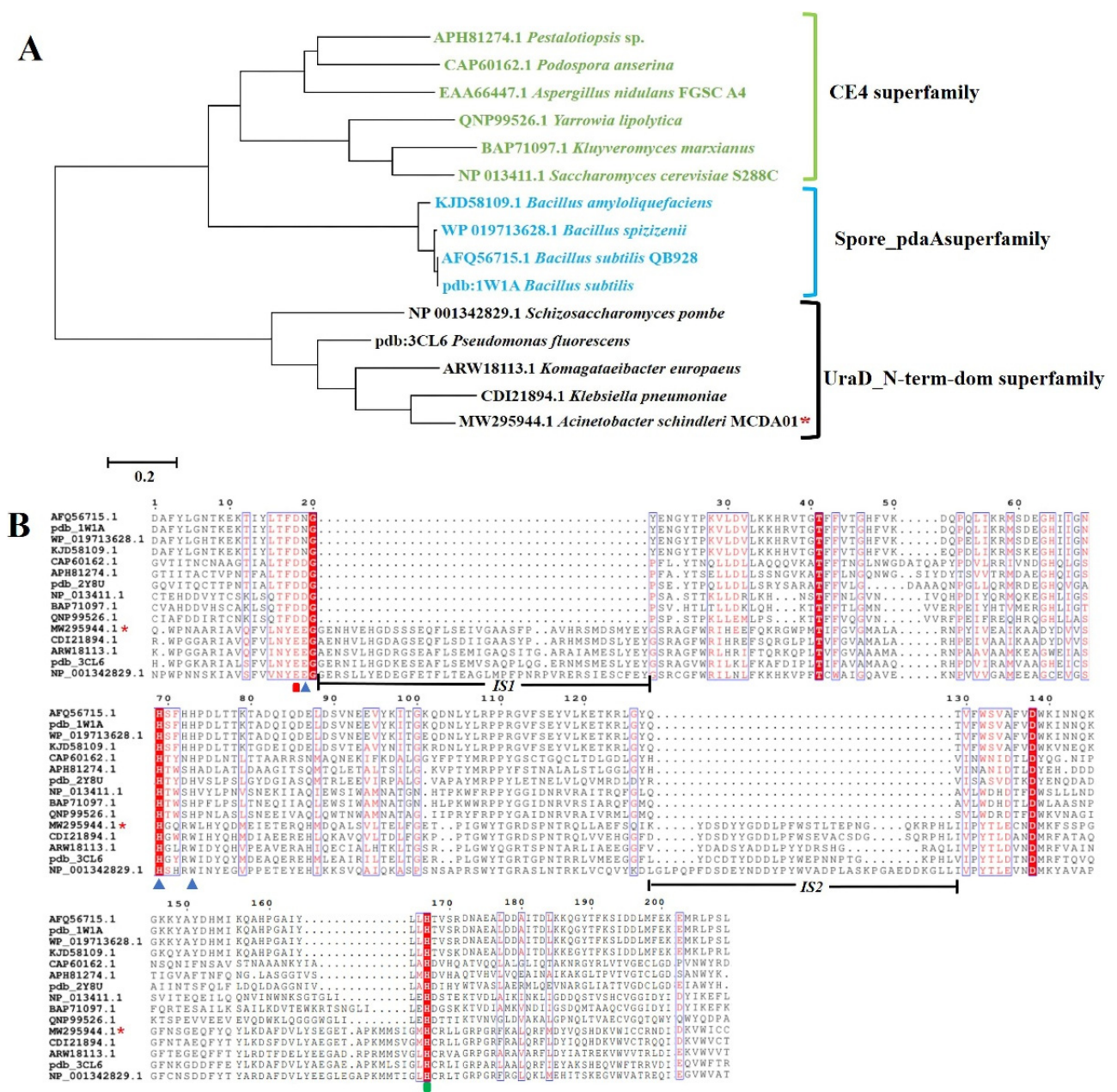


**Figure 3.** Bioinformatics analysis of AsCDA: (A) phylogenetic analysis of neighbor-joining phylogenetic tree; (B) multiple amino acid sequence alignment: the metal binding triads are indicated with blue triangles; the catalytic base and catalytic acid are indicated with red rectangles and green rectangles, respectively.

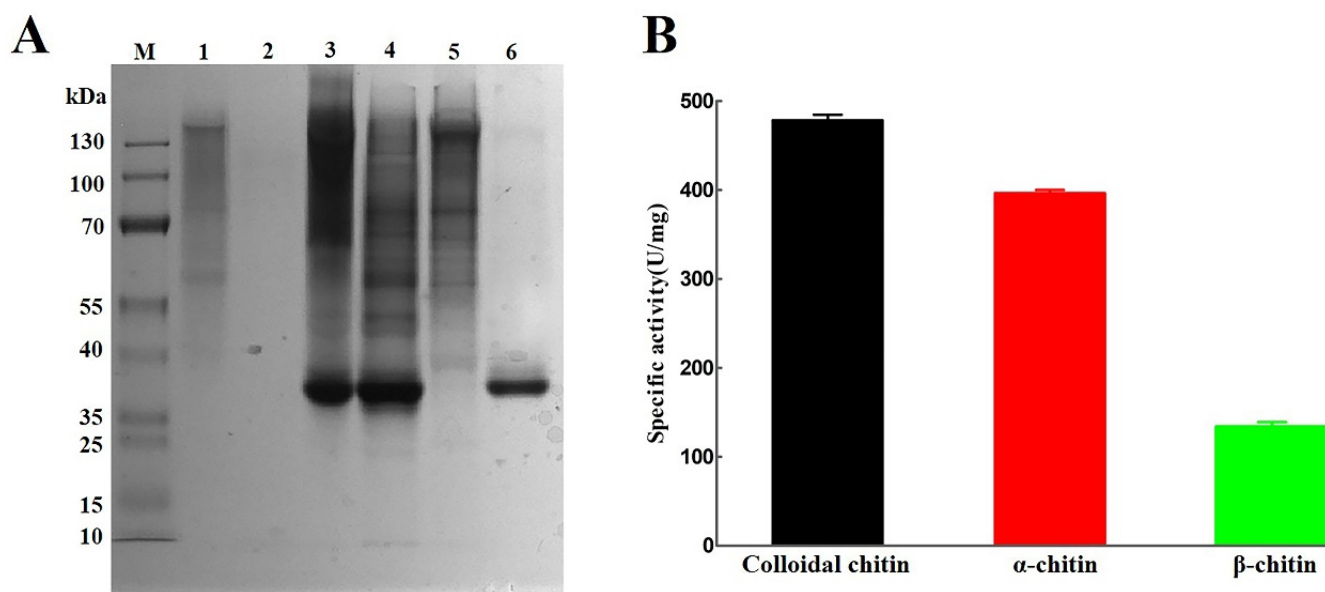


**Figure 4.** Purification and characterization of the recombinant protein AsCDA from *Acinetobacter schindleri* MCDA01: (A) heterologous expression and purification of AsCDA were analyzed by SDS-PAGE on a 12% gel after Coomassie brilliant blue R-250 staining; (B) specific activity of purified AsCDA to colloidal chitin,  $\alpha$ -chitin, and  $\beta$ -chitin. Lane M, proteins marker with standard molecular Masses; lane 1, negative control (empty vector pET-28a); lane 2, Fermentation supernatant from *Escherichia coli* BL21 containing expression vector pET28a-AsCDA induced with IPTG; lane 3, insoluble phase of cellular extracts from *Escherichia coli* BL21 containing expression vector pET28a-AsCDA induced with IPTG; lane 4, soluble phase of cellular extracts from *Escherichia coli* BL21 containing expression vector pET28a-AsCDA induced with IPTG; lane 5, effluent fractions when all proteins were washed clean with elution 80 mM imidazole conc; lane 6, purified AsCDA with elution 300 mM imidazole.

### 2.5. Deacetylation of Crystalline Chitin Catalyzed by Chitin Deacetylase AsCDA

To determine characterized microstructure changes, chitosan,  $\alpha$ -chitin, and AsCDA-Ch were performed for Fourier transform infrared spectroscopy (FT-IR) and scanning electron microscope (SEM). The results of SEM, as in Figure 5, show that untreated  $\alpha$ -chitin was large dense particles stacked in a layered structure whose surface compactly arrange a crystalline microfibril structure, which was compact, rough, and texture. The bulk structure of AsCDA-Ch, however, was severely damaged. Holes and dense rifts were observed on the surface of AsCDA-Ch and its fibers became blurred and indistinct and exhibited a less well-defined interface with separated sheets. The particle state of AsCDA-Ch was similar to chitosan, and was obviously different from  $\alpha$ -chitin. The microstructure images of  $\alpha$ -chitin and chitosan by SEM were reported in previous studies, which further verified that deacetylation of  $\alpha$ -chitin by AsCDA was similar to chitosan [35–37]. The reason for microstructure changes in  $\alpha$ -chitin treated by AsCDA was the reduction in acetyl group content, which caused the intramolecular and molecular structure to be destroyed or weakened [38].

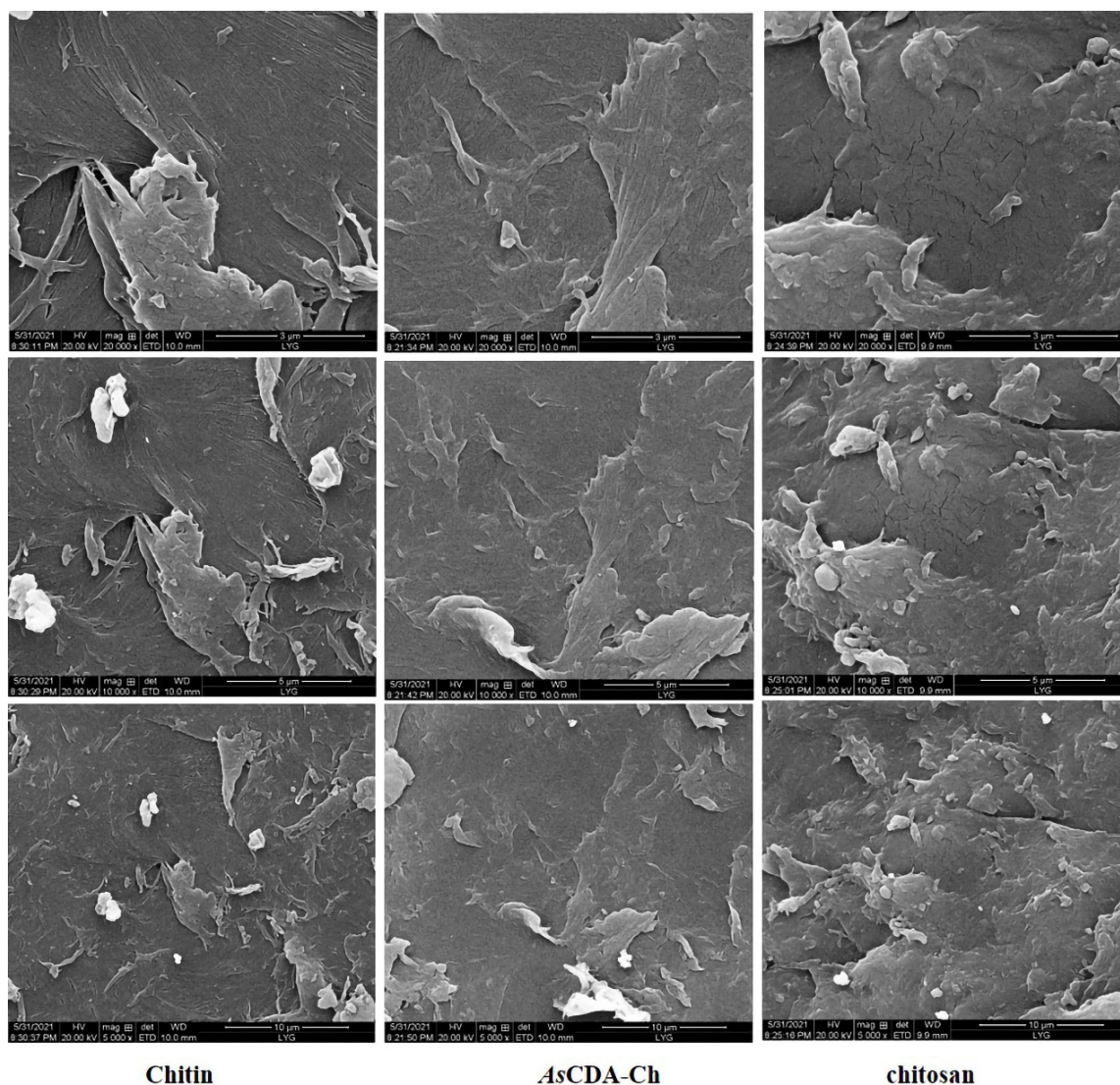


**Figure 5.** SEM images of untreated chitin, chitin treated by AsCDA, and chitosan with magnificant  $\times 20,000$  times,  $\times 10,000$  times, and  $\times 5000$  times.

The comparative analysis results of chitosan,  $\alpha$ -chitin, and AsCDA-Ch by FT-IR showed that the structure of the three samples was basically the same, according to the similarity of the peak position and absorbance. The amide I, II, and III bands of the characteristic peaks were observed at  $1655$ ,  $1560$ , and  $1314$   $\text{cm}^{-1}$  in the FT-IR spectrum, and the peak position of  $1655$   $\text{cm}^{-1}$  indicated that the samples were deacetylated products of  $\alpha$ -type chitin (Figure 6A) [39]. From the absorption bands at  $1655$   $\text{cm}^{-1}$  (amide I) and  $3450$   $\text{cm}^{-1}$  (-OH group) emerged the displacement of the absorption peak in different chitin samples. The  $A_{1655}/A_{3450}$  ratio linear with the degree of deacetylation of chitin was used to calculate the degree of deacetylation (DD) of samples [40]. The DD of the samples was determined on the basis of the  $A_{1655}/A_{3450}$  value from FT-IR results, the degree of deacetylation of  $\alpha$ -chitin, AsCDA-Ch, and chitosan were 25.44%, 88.49%, and 97.54%, respectively (Figure 6B). AsCDA removed 63.05% of the acetyl groups for  $\alpha$ -chitin pretreated for 12 h, and the degree of deacetylation did not change with the increase in treatment time (Figure S3). The results indicated that the enzymatic hydrolysis of AsCDA resulted in the release of an acetyl group and increased the degree of deacetylation of  $\alpha$ -chitin. Compared to the NaCDA from *Nitratireductor aquimarinus* MCDA3-3 studied by our group, the AsCDA showed a significant improvement in reaction time and substrate concentration of the catalytic preparation of chitosan [35]. Chitosan was the deacetylated derivative

of chitin with a high rate of deacetylation higher than 55% [2]. AsCDA has the highest activity toward deacetylation of crystalline chitin and it removes the acetyl group content of crystalline chitin, which had not been pretreated through various physical and chemical methods until this current study (see Supplementary Figure S1) (Figure 7). The enzymatic method is a promising alternative to these traditional physical and chemical methods to promote the chitosan industrial technology upgrade and quality improvement [7]. AsCDA is a potent chitin decomposer to catalyze chitin deacetylation to prepare chitosan and realize the value-added utilization of chitin biological resources.

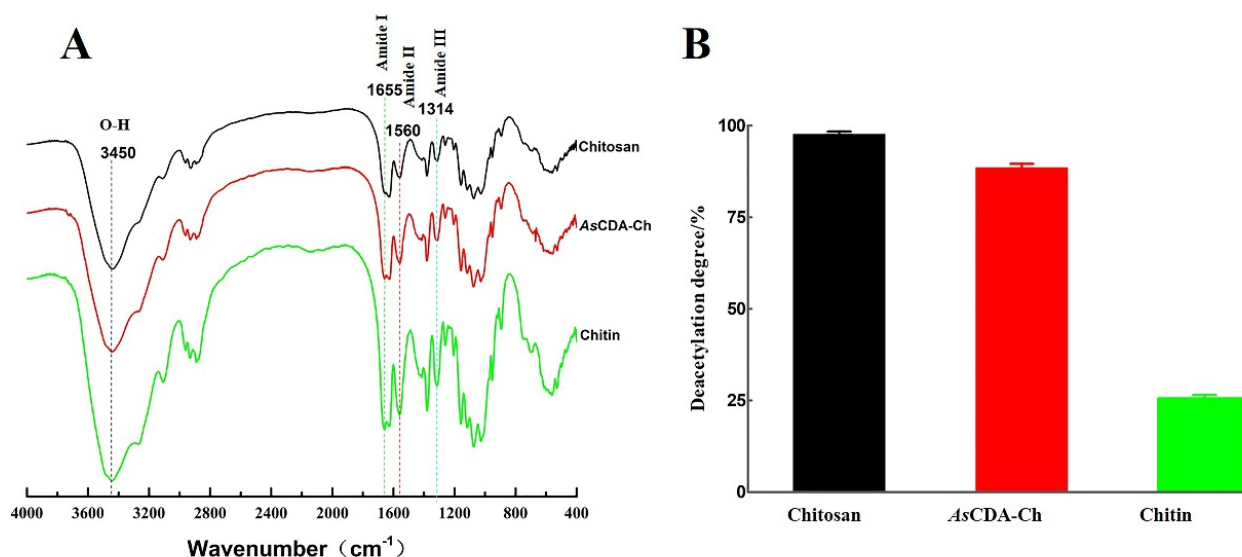


**Figure 6.** FT-IR spectra and determination of the degree of deacetylation of chitosan (black), AsCDA treated chitin (red) and chitin (green): (A) FT-IR spectra; (B) determination of the degree of deacetylation.



**Figure 7.** Simplified diagram of AsCDA to catalyze crystalline chitin deacetylation to prepare chitosan.

### 3. Materials and Methods

#### 3.1. Materials

*Acinetobacter schindleri* MCDA01 (CGMCC NO.13539)-producing chitin deacetylase was isolated from marine mud collected from Yanwei Harbor (34°29'0" N, 119°47'0" E), Lianyungang City, China, which was laboratory preservation strains [11]. Operationally, the medium for the cell growth of *A. schindleri* MCDA01 was a 2216E broth at 20 °C and 180 rpm for 48 h. The  $\alpha$ -chitin was kindly provided by Professor Fan Yimin from Nanjing Forestry University, which was purified from swimming crab (*Portunus trituberculatus*) shells collected from Nantong, a seaside city in Jiangsu Province, China. Chitosan was the degree of deacetylation greater than 95% and average molecular weight (MW) of approximately  $2 \times 10^5$ , which was purchased from Sangon Biotech (Shanghai, China). All other reagents and solvents were analytical grade.

### 3.2. Isolation, Sequencing, and De Novo Assembly of the *Acinetobacter schindleri* MCDA01 Genome

The genomic DNA was extracted by Bacteria Genomic DNA Extraction Kit (TaKaRa, Dalian, China) according to the manufacturer's recommended protocol. Sequencing libraries were generated using a Next Ultra DNA Library Prep Kit for Illumina (New England Biolabs Ltd). The library quality was assessed on the Qubit@ 2.0 Fluorometer (Thermo Scientific) and Agilent Bioanalyzer 2100 system. Subsequently, the libraries with high-quality reads were sequenced using a HiSeq 2500 sequence platform provided by the Illumina company and PE125 strategies. A preliminary assembly of the filtered valid data was performed using SOAPdenovo2 (v.2.04.4; SOAPdenovo2, RRID: SCR\_014986) [41–43]. Whole-genome data of *A. schindleri* MCDA01 was finally submitted to GenBank under accession number CP076603, Bioproject PRJNA733816, and Biosample SAMN19459915.

### 3.3. Gene Prediction and Annotation

After obtaining the whole-genome data of *A. schindleri* MCDA01, genes were predicted using a GeneMarkS v.4.28 (<http://topaz.gatech.edu/GeneMark/> (accessed on 14 July 2022)) [44]. The function of putative coding sequences (CDs) was annotated via local BLAST searches against NCBI NR and SwissProt databases. The genome blast search (E value less than  $1E-5$ , minimum alignment length  $\geq 40\%$ , matching similarity  $\geq 40\%$ ) was deposited in diverse protein databases, including the Kyoto Encyclopedia of Genes and Genomes (KEGG) ([http://www.kegg.jp/kegg/tool/annotate\\_sequence.html](http://www.kegg.jp/kegg/tool/annotate_sequence.html) (accessed on 14 July 2022)) for the metabolic pathways, Non-Redundant Protein Database (NR, <ftp://ftp.ncbi.nih.gov/blast/db/FASTA/nr.gz> (accessed on 14 July 2022)) for protein alignments, the SwissProt ([ftp://ftp.ebi.ac.uk/pub/databases/uniprot/knownledgebase/uniprot\\_sprot.fasta.gz](ftp://ftp.ebi.ac.uk/pub/databases/uniprot/knownledgebase/uniprot_sprot.fasta.gz) (accessed on 14 July 2022)) for mapping the gene-ontology terms, Eucaryotic Orthologous Groups (KOG) for eukaryotic clusters of orthologues, and Gene Ontology (GO, <http://www.geneontology.org/> (accessed on 14 July 2022)) for annotation of the homologous genes and their function, location of cellular components, and biological processes [25,45–49].

### 3.4. Comparative Genome Analysis and Gene Mining of Chitin Deacetylase

To determine the diversity and strain-specific features in *A. schindleri* MCDA01, the pan-genome was analyzed and searched for orthologous genes in the genome of different bacterial strains (*Acinetobacter schindleri* MCDA01, *Acinetobacter schindleri* CIP107287, *Acinetobacter schindleri* ACE, *Bacillus anthracis* Ames, and *Bacillus cereus* ATCC14579, genome information see Supplementary Table S2) with the software package GET\_HOMOLOGUES v3.2.1, which can cluster homologous gene families using the bidirectional best-hit, COG triangles, or OrthoMCL v2.0 clustering algorithms [50–52]. For *Acinetobacter schindleri* CIP107287 and *A. schindleri* ACE, the most closely related to strain *A. schindleri* MCDA01, there were no known reports on producing chitin deacetylase [53,54]. *Bacillus anthracis* Ames and *B. cereus* ATCC14579, producing chitin deacetylase, were complete draft genomes [55,56]. The whole genome synteny between the genome pairs was performed by using the MUMmer-4.0.0beta2 with the 'mum' parameter [57]. In our previous studies, the molecular mass of natural chitin deacetylase was approximately 31 kDa produced by *A. schindleri* MCDA01, which was an important basis for the gene mining of AsCDA [11]. The putative CDAs were identified using a dbCAN2 meta-server for annotation of carbohydrate-active enzymes (CAZymes) [45]. A DNAMAN v9.0.1.116 (<https://www.lynnon.com/index.html>) was used for amino acid sequence alignment and conservative domain analysis. Phylogenetic analysis indicating the relationship of AsCDA to other chitosanases was performed using MEGA 6 software (see Supplementary File).

### 3.5. Heterologous Expression and Purification of AsCDA in *Escherichia coli* BL21

The cDNA of the AsCDA gene was amplified by PCR using the AsCDA1-F (*Bam*HI:GGATCCACAACCTGCTTACTTACGCGGA) and AsCDA1-R (*Hind*III:AAGCCTGTCCTGGTGCGCAGGAAAATG), verified by DNA sequencing, cloned into the pET-28a expression vector and transformed into *Escherichia coli* BL21 (TransGen Biotech, Beijing, China). The expression of the recombinant AsCDA was induced by the addition of isopropyl b-D-thiogalactoside (IPTG, final concentration of 1mM) in Luria–Bertani medium (LB medium, containing 50 ng/mL kanamycin) [58]. After overnight induction at 16 °C, the bacterial cells were collected, resuspended in lysis solution, and sonicated for 30 min. The sediment and supernatant were collected after centrifugation for 20 min (4 °C, 12,000 rpm/min). Recombinant AsCDA was purified by the AKTA-purifier protein purification system and Histidine Ni-Sepharose™ Fast Flow, analyzed by SDS-PAGE on a 12% gel after Coomassie brilliant blue R-250 staining. Protein concentration was determined by the bicinchoninic acid method using BSA as a standard.

### 3.6. Enzyme Assay of AsCDA

The enzymatic activity assay of AsCDA was performed as Acetic Acid Assay Kit (Acetate kinase analyzer format, Megazyme, Republic of Ireland) described by Bergmeyer with modification [59]. The Standard curve of acetic acid with  $\Delta A_{340}$  was drawn for enzyme assay of AsCDA (Figure S2). The reaction mixture of 2 mg  $\alpha$ -chitin and 10  $\mu$ L AsCDA (2.11  $\mu$ g/ $\mu$ L) was added to 190  $\mu$ L phosphate buffer (pH 7.0) and incubated at 30 °C for 30 min; the enzyme reaction was terminated by boiling at 100 °C for 10 min in a sealed tube prior. The supernatant was collected by centrifugation at 12,000 rpm for 5 min, and the amount of acetic acid in 10  $\mu$ L supernatant was determined to calculate the enzyme activity through the  $A_{340}$  according to the assay procedure of the Acetic Acid Assay Kit. The minimum differential absorbance of the Acetic Acid Assay Kit was 0.005 absorbance unit, which was equivalent to 0.063 mg/L acetic acid in the sample solution. One unit of AsCDA activity was defined as the amount of enzyme required to catalyze the release of 1 $\mu$ mol acetic acid per minute.

### 3.7. Scanning Electron Microscope Observation of Deacetylation Effect

Chitosan,  $\alpha$ -chitin, and  $\alpha$ -chitin treated by AsCDA (AsCDA-Ch) were characterized microstructure changes by Scanning electron microscopy (Alexandridis, Ghasemi, Furlani, & Tsianou). AsCDA-Ch was a final concentration of 30 g/L chitin pretreated by AsCDA enzyme solution with 50 mM phosphate buffer with shaking fermentation at 30 °C for 12 h (treatment times were set at 0 h, 2 h, 4 h, 6 h, 8 h, 10 h, 12 h, 14 h, 16 h, 18h, 22 h, and 24 h. After 12 h, the degree of deacetylation did not change with the increase in treatment time). All samples were dried to a constant weight at 100 °C and were respectively adhered to the metal sample stage with a conductive adhesive, and a metal film was sprayed in a vacuum evaporator and then observed under a scanning electron microscope at 20 kV [19,37].

### 3.8. Deacetylation Was Measured by Infrared Spectroscopy

Chitosan,  $\alpha$ -chitin, and AsCDA-Ch carried out an infrared spectrometer in a wavenumber region of 400 to 4000  $\text{cm}^{-1}$  using FT-IR spectra (Nicolet-iS10), which was based on previously described work by Chai et al. [35]. In the FT-IR spectrum of the enzymatic chitin, the absorption bands at 1659 $^{-1}$ , 1560 $^{-1}$ , and 1314  $\text{cm}^{-1}$ , respectively, were the amide I, II, and III bands of the characteristic peaks of acetamido groups, and the absorbance bands at 1655  $\text{cm}^{-1}$  and 3450  $\text{cm}^{-1}$  used to determinate of the degree of deacetylation [60,61]. The difference in DD before ( $\alpha$ -chitin) and after (AsCDA-Ch) enzyme treatment of AsCDA toward  $\alpha$ -chitin was the removed acetyl groups. Infrared determination of the degree of deacetylation calculation formula:

$$DD = \left( 1 - \frac{A_{1655}/A_{3450}}{1.33} \right) \times 100 \quad (1)$$

### 3.9. Statistical Analyses

All tests were performed in triplicate and data were presented as the mean  $\pm$  SE. One-way ANOVA and Duncan's multiple range tests were used to test for variance and significant differences using the SPSS software (version 26.0).

## 4. Conclusions

Chitosan is a biodegradable, biocompatible, and nontoxic aminopolysaccharide, which is widely used in food chemistry as an emulsifier, flocculant, and functional food additive. Chitin deacetylases catalyzed the crystal chitin deacetylation to prepare chitosan, which was a safe, controllable, and environmentally friendly process to replace the traditional current chemical methods. The low catalytic activity of CDAs for the deacetylation of crystalline chitin, however, did not meet the demand for the industrial production of chitosan. Thus, appropriate CDA should be explored to improve the efficiency of enzymatic hydrolysis to crystalline chitin for chitosan production. In this study, AsCDA, a member of the uraD\_N-term-dom superfamily, was mined uniquely through the *A. schindleri* MCDA01 genome database of bioinformatics analysis. AsCDA was biochemically characterized in *E. coli* BL21, which has a high activity rate and deacetylation reaction for crystalline chitin. The results of FT-IR and SEM confirmed that the enzymatic hydrolysis of AsCDA released the acetyl group and increased the degree of deacetylation of crystalline chitin, which removed 63.05% of the acetyl groups for crystalline chitin and prepared industrial chitosan in 12 h. AsCDA is a potent chitin decomposer to catalyze chitin deacetylation to prepare chitosan, and these findings will hopefully realize the effective conversion of chitin bioresources into their valuable derivatives: chitin nanofibers, chitosan, and chitoooligosaccharides. The study on crystal structures of AsCDA will be a suitable method to elucidate the molecular mechanism of the deacetylation of long-chain chitin catalyzed by CDAs, which, in the future, will be the next scientific research subject of our research group.

**Supplementary Materials:** The following supporting information can be downloaded at: <https://www.mdpi.com/article/10.3390/molecules27165345/s1>, Figure S1: Circular graph of the *Acinetobacter schindleri* MCDA01 complete genome; Figure S2: Standard curve of acetic acid for enzyme assay of AsCDA; Figure S3: The determination of the degree of deacetylation of  $\alpha$ -chitin treated by AsCDA with different time points; Table S1: CDAs with characterized activity on crystalline chitin; Table S2: Chitin degrading enzymes in *Acinetobacter schindleri* MCDA01 identified by the CAZy database; Table S3: General genome features of seventeen strains in this study.

**Author Contributions:** Data curation, G.Y. and J.A.; formal analysis, Y.F.; funding acquisition, G.Y.; investigation, Y.W.; methodology, Y.W., J.L. and R.Z.; project administration, G.Y., Y.F., X.H. and S.L.; software, J.A.; writing—original draft, G.Y., Y.W. and S.L.; writing—review & editing, G.Y. and Y.F. All authors have read and agreed to the published version of the manuscript.

**Funding:** This work was supported by the National Natural Science Foundation of China (31772016, 32102270), the Priority Academic Program Development of Jiangsu Higher Education Institutions, the Key Natural Science Foundation of the Jiangsu Higher Education Institutions of China (20KJA550001), the National Natural Science Foundation of Jiangsu Ocean University (KQ20041, KQ20052), the Project“333” of Jiangsu Province, Postgraduate Research and Practice Innovation Program of Jiangsu Province (KYCX20\_2883), Open-end Funds of Jiangsu Institute of Marine Resources Development (JSIMR202024) and Open-end Funds of Jiangsu Key Laboratory of Marine Bioresources and Environment (SH20211210).

**Conflicts of Interest:** The authors declare no conflict of interest.

## References

1. Yan, N.; Chen, X. Sustainability: Don't waste seafood waste. *Nature* **2015**, *524*, 155–157. [[CrossRef](#)] [[PubMed](#)]
2. Arnold, N.D.; Bruck, W.M.; Garbe, D.; Bruck, T.B. Enzymatic modification of native chitin and conversion to specialty chemical products. *Mar. Drugs* **2020**, *18*, 93. [[CrossRef](#)] [[PubMed](#)]
3. Karrer, P.; Hofmann, A. Polysaccharide xxxix. Über den enzymatischen abbau von chitin und chitosan I. *Helv. Chim. Acta* **1929**, *12*, 616–637. [[CrossRef](#)]

4. Aspras, I.; Jaworska, M.M.; Gorak, A. Kinetics of chitin deacetylase activation by the ionic liquid [Bmim][Br]. *J. Biotechnol.* **2017**, *251*, 94–98. [[CrossRef](#)]
5. Deringer, V.L.; Englert, U.; Dronskowski, R. Nature, strength, and cooperativity of the hydrogen-bonding network in alpha-chitin. *Biomacromolecules* **2016**, *17*, 996–1003. [[CrossRef](#)]
6. Tsigos, I.; Martinou, A.; Kafetzopoulos, D.; Bouriotis, V. Chitin deacetylases: New, versatile tools in biotechnology. *Trends Biotechnol.* **2000**, *18*, 305–312. [[CrossRef](#)]
7. Kaczmarek, M.B.; Struszczyk-Swita, K.; Xiao, M.; Szczesna-Antczak, M.; Antczak, T.; Gierszewska, M.; Steinbuchel, A.; Daroch, M. Polycistronic expression system for *Pichia pastoris* composed of chitino- and chitosanolytic enzymes. *Front Bioeng. Biotechnol.* **2021**, *9*, 710922. [[CrossRef](#)]
8. Casadidio, C.; Peregrina, D.V.; Gigliobianco, M.R.; Deng, S.; Censi, R.; Di Martino, P. Chitin and chitosans: Characteristics, eco-friendly processes, and applications in cosmetic science. *Mar. Drugs* **2019**, *17*, 369. [[CrossRef](#)]
9. Muxika, A.; Etxabide, A.; Uranga, J.; Guerrero, P.; de la Caba, K. Chitosan as a bioactive polymer: Processing, properties and applications. *Int. J. Biol. Macromol.* **2017**, *105*, 1358–1368. [[CrossRef](#)]
10. Park, B.K.; Kim, M.M. Applications of chitin and its derivatives in biological medicine. *Int. J. Mol. Sci.* **2010**, *11*, 5152–5164. [[CrossRef](#)]
11. Ye, W.; Ma, H.; Liu, L.; Yu, J.; Lai, J.; Fang, Y.; Fan, Y. Biocatalyzed route for the preparation of surface-deacetylated chitin nanofibers. *Green Chem.* **2019**, *21*, 3143–3151. [[CrossRef](#)]
12. Yuan, X.; Zheng, J.; Jiao, S.; Cheng, G.; Feng, C.; Du, Y.; Liu, H. A review on the preparation of chitosan oligosaccharides and application to human health, animal husbandry and agricultural production. *Carbohydr. Polym.* **2019**, *220*, 60–70. [[CrossRef](#)]
13. Blair, D.E.; Schuttelkopf, A.W.; Macrae, J.I.; van Aalten, D.M. Structure and metal-dependent mechanism of peptidoglycan deacetylase, a streptococcal virulence factor. *Proc. Natl. Acad. Sci. USA* **2005**, *102*, 15429–15434. [[CrossRef](#)]
14. Younes, I.; Rinaudo, M. Chitin and chitosan preparation from marine sources. Structure, properties and applications. *Mar. Drugs* **2015**, *13*, 1133–1174. [[CrossRef](#)]
15. Yang, W.J.; Xu, K.K.; Yan, Y.; Li, C.; Jin, D.C. Role of chitin deacetylase 1 in the molting and metamorphosis of the cigarette beetle *Lasioderma serricorne*. *Int. J. Mol. Sci.* **2020**, *21*, 2449. [[CrossRef](#)]
16. Liu, X.; Zhang, J.; Zhu, K.Y. Chitin in arthropods: Biosynthesis, modification, and metabolism. *Adv. Exp. Med. Biol.* **2019**, *1142*, 169–207.
17. Araki, Y.; Ito, E. A pathway of chitosan formation in *Mucor rouxii*. Enzymatic deacetylation of chitin. *Eur. J. Biochem.* **1975**, *55*, 71–78. [[CrossRef](#)]
18. Yang, G.; Hou, X.; Lu, J.; Wang, M.; Wang, Y.; Huang, Y.; Liu, Q.; Liu, S.; Fang, Y. Enzymatic modification of native chitin and chitin oligosaccharides by an alkaline chitin deacetylase from *Microbacterium esteraromaticum* MCDA02. *Int. J. Biol. Macromol.* **2022**, *203*, 671–678. [[CrossRef](#)]
19. Shrestha, B.; Blondeau, K.; Stevens, W.F.; Hegarat, F.L. Expression of chitin deacetylase from *Colletotrichum lindemuthianum* in *Pichia pastoris*: Purification and characterization. *Protein Expr. Purif.* **2004**, *38*, 196–204. [[CrossRef](#)]
20. Zhu, X.Y.; Zhao, Y.; Zhang, H.D.; Wang, W.X.; Cong, H.H.; Yin, H. Characterization of the specific mode of action of a chitin deacetylase and separation of the partially acetylated chitosan oligosaccharides. *Mar. Drugs* **2019**, *17*, 74. [[CrossRef](#)]
21. Win, N.N.; Stevens, W.F. Shrimp chitin as substrate for fungal chitin deacetylase. *Appl. Microbiol. Biotechnol.* **2001**, *57*, 334–341. [[PubMed](#)]
22. Yamada, M.; Kurano, M.; Inatomi, S.; Taguchi, G.; Okazaki, M.; Shimosaka, M. Isolation and characterization of a gene coding for chitin deacetylase specifically expressed during fruiting body development in the basidiomycete *Flammulina velutipes* and its expression in the yeast *Pichia pastoris*. *FEMS Microbiol. Lett.* **2008**, *289*, 130–137. [[CrossRef](#)] [[PubMed](#)]
23. Liu, Z.; Gay, L.M.; Tuveng, T.R.; Agger, J.W.; Westereng, B.; Mathiesen, G.; Horn, S.J.; Vaaje-Kolstad, G.; van Aalten, D.; Eijssink, V. Structure and function of a broad-specificity chitin deacetylase from *Aspergillus nidulans* FGSC A4. *Sci. Rep.* **2017**, *7*, 1746. [[CrossRef](#)] [[PubMed](#)]
24. Ma, Q.; Gao, X.; Tu, L.; Han, Q.; Zhang, X.; Guo, Y.; Yan, W.; Shen, Y.; Wang, M. Enhanced chitin deacetylase production ability of *Rhodococcus equi* CGMCC14861 by co-culture fermentation with *Staphylococcus* sp. MC7. *Front. Microbiol.* **2020**, *11*, 592477. [[CrossRef](#)]
25. Wang, Y.; Song, J.Z.; Yang, Q.; Liu, Z.H.; Huang, X.M.; Chen, Y. Cloning of a heat-stable chitin deacetylase gene from *Aspergillus nidulans* and its functional expression in *Escherichia coli*. *Appl. Biochem. Biotechnol.* **2010**, *162*, 843–854. [[CrossRef](#)]
26. Kang, L.; Chen, X.; Zhai, C.; Ma, L. Synthesis and high expression of chitin deacetylase from *Colletotrichum lindemuthianum* in *Pichia pastoris* GS115. *J. Microbiol. Biotechnol.* **2012**, *22*, 1202–1207. [[CrossRef](#)]
27. Blair, D.E.; Hekmat, O.; Schuttelkopf, A.W.; Shrestha, B.; Tokuyasu, K.; Withers, S.G.; van Aalten, D.M. Structure and mechanism of chitin deacetylase from the fungal pathogen *Colletotrichum lindemuthianum*. *BMC Biochem.* **2006**, *45*, 9416–9426. [[CrossRef](#)]
28. Dsouza, M.; Taylor, M.W.; Turner, S.J.; Aislabie, J. Genomic and phenotypic insights into the ecology of *Arthrobacter* from antarctic soils. *BMC Genom.* **2015**, *16*, 36. [[CrossRef](#)]
29. Yadav, S.; Dubey, S.K. Cellulose degradation potential of *Paenibacillus lautus* strain BHU3 and its whole genome sequence. *Bioresour. Technol.* **2018**, *262*, 124–131. [[CrossRef](#)]
30. Ma, Q.; Gao, X.; Bi, X.; Tu, L.; Xia, M.; Shen, Y.; Wang, M. Isolation, characterisation, and genome sequencing of *Rhodococcus equi*: A novel strain producing chitin deacetylase. *Sci. Rep.* **2020**, *10*, 4329. [[CrossRef](#)]

31. Ramazzina, I.; Cendron, L.; Folli, C.; Berni, R.; Monteverdi, D.; Zanotti, G.; Percudani, R. Logical identification of an allantoinase analog (puue) recruited from polysaccharide deacetylases. *J. Biol. Chem.* **2008**, *283*, 23295–23304. [[CrossRef](#)]
32. Grifoll-Romero, L.; Pascual, S.; Aragunde, H.; Biarnes, X.; Planas, A. Chitin deacetylases: Structures, specificities, and biotech applications. *Polymers* **2018**, *10*, 352. [[CrossRef](#)]
33. Zhao, Y.; Park, R.D.; Muzzarelli, R.A. Chitin deacetylases: Properties and applications. *Mar. Drugs* **2010**, *8*, 24–46. [[CrossRef](#)]
34. Alfonso, C.; Nuero, O.M.; Santamaria, F.; Reyes, F. Purification of a heat-stable chitin deacetylase from *Aspergillus nidulans* and its role in cell wall degradation. *Curr. Microbiol.* **1995**, *30*, 49–54. [[CrossRef](#)]
35. Chai, J.; Hang, J.; Zhang, C.; Yang, J.; Wang, S.; Liu, S.; Fang, Y. Purification and characterization of chitin deacetylase active on insoluble chitin from *Nitratireductor aquimarinus* MCDA3-3. *Int. J. Biol. Macromol.* **2020**, *152*, 922–929. [[CrossRef](#)]
36. Pareek, N.; Vivekanand, V.; Agarwal, P.; Saroj, S.; Singh, R.P. Bioconversion to chitosan: A two stage process employing chitin deacetylase from *Penicillium oxalicum* SAEM-51. *Carbohydr. Polym.* **2013**, *96*, 417–425. [[CrossRef](#)]
37. Li, J.; Huang, W.C.; Gao, L.; Sun, J.; Liu, Z.; Mao, X. Efficient enzymatic hydrolysis of ionic liquid pretreated chitin and its dissolution mechanism. *Carbohydr. Polym.* **2019**, *211*, 329–335. [[CrossRef](#)]
38. Ma, Q.; Gao, X.; Bi, X.; Han, Q.; Tu, L.; Yang, Y.; Shen, Y.; Wang, M. Dissolution and deacetylation of chitin in ionic liquid tetrabutylammonium hydroxide and its cascade reaction in enzyme treatment for chitin recycling. *Carbohydr. Polym.* **2020**, *230*, 115605. [[CrossRef](#)]
39. Velde, K.K.V.D.; Kiekens, P. Structure analysis and degree of substitution of chitin, chitosan and dibutylchitin by FT-IR spectroscopy and solid state <sup>13</sup>C NMR. *Carbohydr. Polym.* **2004**, *58*, 409–416. [[CrossRef](#)]
40. Peh, K.K.; Khan, T.A.; Ch'Ng, H.S. Mechanical, bioadhesive strength and biological evaluations of chitosan films for wound dressing. *J. Pharm. Pharmaceut.* **2000**, *3*, 303–311.
41. Li, R.; Li, Y.; Kristiansen, K.; Wang, J. Soap: Short oligonucleotide alignment program. *Bioinformatics* **2008**, *24*, 713–714. [[CrossRef](#)]
42. Li, R.; Zhu, H.; Ruan, J.; Qian, W.; Fang, X.; Shi, Z.; Li, Y.; Li, S.; Shan, G.; Kristiansen, K.; et al. De novo assembly of human genomes with massively parallel short read sequencing. *Genome Res.* **2010**, *20*, 265–272. [[CrossRef](#)]
43. Luo, R.; Liu, B.; Xie, Y.; Li, Z.; Huang, W.; Yuan, J.; He, G.; Chen, Y.; Pan, Q.; Liu, Y.; et al. Erratum: Soapdenovo2: An empirically improved memory-efficient short-read de novo assembler. *Gigascience* **2015**, *4*, 30. [[CrossRef](#)]
44. Besemer, J.; Lomsadze, A.; Borodovsky, M. Genemarks: A self-training method for prediction of gene starts in microbial genomes. Implications for finding sequence motifs in regulatory regions. *Nucleic Acids Res.* **2001**, *29*, 2607–2618. [[CrossRef](#)]
45. Zhang, H.; Yohe, T.; Huang, L.; Entwistle, S.; Wu, P.; Yang, Z.; Busk, P.K.; Xu, Y.; Yin, Y. DbcAn2: A meta server for automated carbohydrate-active enzyme annotation. *Nucleic Acids Res.* **2018**, *46*, W95–W101. [[CrossRef](#)]
46. Jungo, F.; Bougueleret, L.; Xenarios, I.; Poux, S. The uniprotkb/swiss-prot tox-prot program: A central hub of integrated venom protein data. *Toxicon* **2012**, *60*, 551–557. [[CrossRef](#)]
47. Magrane, M. Uniprot knowledgebase: A hub of integrated protein data. *Database* **2011**, *2011*, r9. [[CrossRef](#)]
48. Koonin, E.V.; Fedorova, N.D.; Jackson, J.D.; Jacobs, A.R.; Krylov, D.M.; Makarova, K.S.; Mazumder, R.; Mekhedov, S.L.; Nikolskaya, A.N.; Rao, B.S.; et al. A comprehensive evolutionary classification of proteins encoded in complete eukaryotic genomes. *Genome Biol.* **2004**, *5*, R7. [[CrossRef](#)]
49. Yang, G.; Cui, X.; Liu, S.; Lu, J.; Hou, X.; Meng, W.; Wu, B.; Su, Y.; Zhang, H.; Zheng, W.; et al. Effects of dietary *Lactobacillus helveticus* on the growth rate, disease resistance and intestinal health of pond loach (*Misgurnus anguillicaudatus*). *Aquaculture* **2021**, *544*, 737038. [[CrossRef](#)]
50. Vinuesa, P.; Contreras-Moreira, B. Robust identification of orthologues and paralogues for microbial pan-genomics using get\_homologues: A case study of pinca/c plasmids. *Methods Mol. Biol.* **2015**, *1231*, 203–232.
51. Wang, Y.; Coleman-Derr, D.; Chen, G.; Gu, Y.Q. Orthovenn: A web server for genome wide comparison and annotation of orthologous clusters across multiple species. *Nucleic Acids Res.* **2015**, *43*, W78–W84. [[CrossRef](#)] [[PubMed](#)]
52. Li, S.; Tang, Y.; Fang, X.; Qiao, T.; Han, S.; Zhu, T. Whole-genome sequence of *Arthrionium phaeospermum*, a globally distributed pathogenic fungus. *Genomics* **2020**, *112*, 919–929. [[CrossRef](#)] [[PubMed](#)]
53. Sigala, J.C.; Suarez, B.P.; Lara, A.R.; Borgne, S.L.; Bustos, P.; Santamaria, R.I.; Gonzalez, V.; Martinez, A. Genomic and physiological characterization of a laboratory-isolated *Acinetobacter schindleri* ACE strain that quickly and efficiently catabolizes acetate. *Microbiology* **2017**, *163*, 1052–1064. [[CrossRef](#)] [[PubMed](#)]
54. Sigala, J.C.; Quiroz, L.; Arteaga, E.; Olivares, R.; Lara, A.R.; Martinez, A. Physiological and transcriptional comparison of acetate catabolism between *Acinetobacter schindleri* ACE and *Escherichia coli* JM101. *FEMS Microbiol. Lett.* **2019**, *366*, fnz151. [[CrossRef](#)]
55. Read, T.D.; Peterson, S.N.; Tourasse, N.; Baillie, L.W.; Paulsen, I.T.; Nelson, K.E.; Tettelin, H.; Fouts, D.E.; Eisen, J.A.; Gill, S.R.; et al. The genome sequence of *Bacillus anthracis* Ames and comparison to closely related bacteria. *Nature* **2003**, *423*, 81–86. [[CrossRef](#)]
56. Andreou, A.; Giastas, P.; Christoforides, E.; Eliopoulos, E.E. Structural and evolutionary insights within the polysaccharide deacetylase gene family of *Bacillus anthracis* and *Bacillus cereus*. *Genes* **2018**, *9*, 386. [[CrossRef](#)]
57. Khatri, I.; Tomar, R.; Ganesan, K.; Prasad, G.S.; Subramanian, S. Complete genome sequence and comparative genomics of the probiotic yeast *Saccharomyces boulardii*. *Sci. Rep.* **2017**, *7*, 371. [[CrossRef](#)]
58. Yang, G.; Xiu, Y.; Chen, Y.; Bai, L.; Sha, Z. Identification and expression of complement component c8 $\alpha$ , c8 $\beta$  and c8 $\gamma$  gene in half-smooth tongue sole (*Cynoglossus semilaevis*) and c8 $\alpha$  recombinant protein antibacterial activity analysis. *Fish Shellfish Immunol.* **2017**, *72*, 658–669. [[CrossRef](#)]
59. Bergmeyer, H.-U. *Methods of Enzymatic Analysis*; Wiley: Hoboken, NJ, USA, 1974; Volume 4.

- 
60. Hou, X.; Wang, Z.; Sun, J.; Li, M.; Wang, S.; Chen, K.; Gao, Z. A microwave-assisted aqueous ionic liquid pretreatment to enhance enzymatic hydrolysis of eucalyptus and its mechanism. *Bioresour. Technol.* **2019**, *272*, 99–104. [[CrossRef](#)]
  61. Ngo, T.; Ngo, D.N. Effects of low-frequency ultrasound on heterogenous deacetylation of chitin. *Int. J. Biol. Macromol.* **2017**, *104*, 1604–1610. [[CrossRef](#)]